

Kinetic Modelling of Molybdenum-blue Production by *Bacillus* sp. strain Neni-10

Yakasai, M.H. ^{1*} and Manogaran, M. ²

¹Department of Biochemistry, Faculty of Basic Medical Sciences, College of Health Science, Bayero University Kano, P. M. B 3011, Nigeria.

²Department of Biochemistry, Faculty of Biotechnology and Biomolecular Sciences, Universiti Putra Malaysia, 43400 UPM Serdang, Selangor, Malaysia.

*Corresponding author:

Dr. Hafeez Muhammad Yakasai,
Department of Biochemistry, Faculty of Basic Medical Sciences,
College of Health Science, Bayero University, Kano,
P. M. B 3011, Kano State Nigeria.
Tel: +2348034966925
Email: hmyakasai.bch@buk.edu.ng

HISTORY

Received: 4th June 2020
Received in revised form: 30th June 2020
Accepted: 21st July 2020

KEYWORDS

Bacillus sp.
Detoxification
Mo-blue
growth curve
Baranyi-Roberts

ABSTRACT

Kinetic modelling of bacterial reduction process reveals vital parameters like specific reduction rate, hypothetical maximum reduction and deduce whether high substrate (molybdenum) concentration affects the lag phase of the reduction. The commonly used natural logarithmic transformation to linearize the reduction process seems inaccurate as it gives only an approximate value for the specific growth rate. This work for the first time utilized eight different primary models such as Gompertz, Baranyi-Roberts, Logistic, Von Bertalanffy, Richards, Schnute, Buchanan three-phase Huang to obtain values of the kinetic constants that could further be used for secondary modelling. Baranyi-Roberts model was the best model fitting Mo-blue production curve in *Bacillus* sp. strain Neni-10 based on statistical values for RMSE (root-mean-square error), R^2 (adjusted coefficient of determination), AICc (corrected Akaike Information Criterion) BF (bias factor) and AF (accuracy factor). The fitting parameters obtained were lag time (λ), maximal Mo-blue production (Y_{max}) and maximum Mo-blue production rate (μ_m). The use of microbial growth models to get accurate Mo-blue production rate is entirely new to molybdenum reduction (detoxification) process and the kinetic constants obtained could be very useful secondary modelling. This work has revealed the usefulness of these models in modelling bacterial Mo-blue production.

INTRODUCTION

Bacterial growth-associated processes often exhibit a unique phase where specific growth rate begins at zero value producing a lag time (λ), after which it accelerates to a maximal value (μ_{max}) for a certain time. The sigmoid-shaped lag period has been argued to be due to the bacterial cells adjusting to the new environment and gearing their growth mechanism in a vegetative phase particularly during storage. The adjustment period (lag period) has been suggested as a transient period that links two autonomous systems. The introduction of the lag time or parameter is mainly for convenience rather than having a mechanistic interpretation [1]. It was hypothesized that, each bacterial cell in the initial inocula, would have different growth rates, that could show nonlinear distribution as earlier suggested [1,2].

Molybdenum as ubiquitous heavy metal has numerous industrial uses including as corrosion resistant steel, lubricant, alloying agent, anti-freeze in automobile engine and as molybdenum disulphide. These industrial wide spread applications of molybdenum have resulted in pollution of several water bodies worldwide as earlier reported in Tyrol in Austria, Tokyo Bay in Japan and the Black Sea, where hundreds of ppm molybdenum level were found [3]. Additionally, significant sewage sludge pollution that poses a health hazard was terrestrially reported [3]. Molybdenum in elemental form or in different chemical combination was reported to be toxic to ruminants particularly cow at concentrations as low as parts per million (ppm) [4,5]. The perceived lower human molybdenum toxicity case compared to other heavy metals like chromium, mercury, and cadmium is attributed to less attention been paid and has resulted in little works on molybdenum detoxification (bioreduction) process. To date, a number of molybdenum-reducing bacteria have been

locally isolated [6–13] with few exceptional commercial strains [14–17]. However, with recent data on molybdenum toxicity by inhibiting spermatogenesis and arresting embryogenesis in catfish and mice at levels as low as ppm [18,19] calls for more works on microbial molybdenum detoxification.

The kinetic studies on microbial Mo-blue production have been explored [20,21], however, these works linearize the Mo-blue production over time profile to obtain the specific growth rate for further secondary modelling. Perhaps the benefits of nonlinear regression analysis for the Mo-blue production have been described. Therefore, this work focus on evaluating the available models such as Gompertz [22,23], Logistic [23,24], Baranyi-Roberts [25], Richards [23,26], Schnute [23], Buchanan three-phase [27], Von Bertalanffy [28,29] and the recently Huang model [30] (Table 1) to model Mo-blue production by *Bacillus* sp. strain Neni-10.

MATERIALS AND METHODS

Maintenance of the Molybdenum-reducing bacterium

The bacterium previously isolated, identified and characterized by Mansur *et al.* [11] was maintained on low phosphate agar media (pH 7.0) containing glucose (1%), Na₂MoO₄.2H₂O (0.242%), Na₂HPO₄ (0.071% or 5 mM), (NH₄)₂SO₄ (0.3%), MgSO₄.7H₂O (0.05%), NaCl (0.5%) and yeast extract (0.05%) [9]. Though, glucose was separately autoclaved.

Preparation of resting cells for molybdenum reduction characterization

Static culture using resting cells in a microplate was used to Monitor the Mo-blue production at various sodium molybdate concentration [31]. Cells grown in 1 L high phosphomolybdate media (HPM=100 mM phosphate) on orbital shaker (150 rpm) at room temperature overnight were harvested by centrifuging at 12,000 x g for 10 minutes. The pellet was then rinsed three times with 20 ml of low phosphate media (LPM) devoid molybdenum to remove suspended cells and residual phosphate to an absorbance of approximately 1.00 at 600 nm. The higher concentration (100 mM) was found to strongly inhibit Mo-blue production [6,21,32–38]. Sterically 180 µL of various concentrations of sodium molybdate dispensed into each well of a sterile microplate, followed by the inoculation with 20 µL from a stock culture to initiate Mo-blue production. A sterile sealing tape that allows gas exchange (Corning® microplate) was used to seal the plate and incubated at room temperature. Periodically, absorbance at 750 nm was read using BioRad microtiter plate reader (Richmond, CA, Model No. 680) to monitor the Mo-blue production from the media using a specific extinction coefficient of 11.69 mM⁻¹.cm⁻¹ [39].

Determining the kinetic parameters of Mo-blue production

Data fitting

CurveExpert Professional software (Version 1.6) was used to conduct nonlinear regression to fit-in the growth data involving the Marquardt algorithm that minimizes sums of square of residuals. This lookup approach minimizes the sum of squares of the differences between the observed and predicted values. Input into the software can be manually or automatically programmed to calculate initial values of parameters. The estimation of µ_m involves the steepest ascent search of the curve among four datum points. While λ estimation was conducted by determining the intersection of this line with x axis. Estimation of asymptote (A) was finally done by taking the final datum point.

Table 1. Models used to model Mo-blue production *Bacillus* sp. strain Neni-10.

Model	p	Equation
Modified Logistic	3	$y = \frac{A}{\left\{ 1 + \exp \left[\frac{4\mu_m}{A} (\lambda - t) + 2 \right] \right\}}$
Modified Gompertz	3	$y = A \exp \left\{ - \exp \left[\frac{\mu_m e}{A} (\lambda - t) + 1 \right] \right\}$
Modified Richards	4	$y = A \left\{ 1 + v \exp(1 + v) \exp \left[\frac{\mu_m}{A} (1 + v) \left(1 + \frac{1}{v} \right) (\lambda - t) \right] \right\}^{-1}$
Modified Schnute	4	$y = \left(\mu_m \frac{(1 - \beta)}{\alpha} \right) \left[\frac{1 - \beta \exp(\alpha \lambda + 1 - \beta - \alpha t)}{1 - \beta} \right]^{\frac{1}{\beta}}$
Baranyi-Roberts	4	$y = A + \mu_m x + \frac{1}{\mu_m} \ln \left(e^{-\mu_m x} + e^{-h_0} - e^{-\mu_m x - h_0} \right) - \ln \left[1 + \frac{e^{\mu_m x} + \frac{1}{\mu_m} \ln \left(e^{-\mu_m x} + e^{-h_0} - e^{-\mu_m x - h_0} \right)}{e^{(y_{\max} - A)}} \right]$
Von Bertalanffy	3	$y = K \left[1 - \left[1 - \left(\frac{A}{K} \right)^3 \right] \exp \left(- \left(\mu_m x / 3K \right)^{\frac{1}{3}} \right) \right]^3$
Huang	4	$y = A + y_{\max} - \ln \left(e^A + \left(e^{y_{\max}} - e^A \right) e^{-\mu_m B(x)} \right)$ $B(x) = x + \frac{1}{\alpha} \ln \frac{1 + e^{-\alpha(x-\lambda)}}{1 + e^{\alpha \lambda}}$
Buchanan Three-phase linear model	3	Y = A, IF X < LAG Y = A + K(X - λ), IF λ < X <

Note:

- A= Mo-blue lower asymptote;
- µ_m= maximum specific Mo-blue production rate;
- v= affects near which asymptote maximum Mo-blue production occurs.
- λ=lag time
- y_{max}= Mo-blue upper asymptote;
- e = exponent (2.718281828)
- t = sampling time
- α,β, k = curve fitting parameters
- h₀ = a dimensionless parameter quantifying the initial physiological state of the reduction process. The lag time (h⁻¹) can be calculated as h₀=µ_{max}

Statistical analysis

To ascertain if there is significant difference between models with different number of parameters, with regards to the fitness quality of same experimental data, statistics like Root-Mean-Square Error (RMSE), adjusted coefficient of determination (R^2), corrected AICc (Akaike Information Criterion), bias factor (BF) and accuracy factor (AF) could be used.

The RMSE was calculated according to **Eqn. 1**, where n is the number of experimental data, p is the number of parameters assessed by the model, Ob_i is the experimental data and Pd_i are the values predicted by the model. It is predicted that a model with smaller number of parameters will give a smaller RMSE values [40].

$$RMSE = \sqrt{\frac{\sum_{i=1}^n (Pd_i - Ob_i)^2}{n - p}} \quad (\text{Eqn. 1})$$

The quality of fit of a model in a linear regression is assessed using R^2 (coefficient of determination). However, R^2 does not provide comparable analysis in a nonlinear regression where the number of parameters between the models vary, as such adjusted R^2 is used to calculate the quality of the nonlinear models employing equations 2 and 3. According to the formula, S_y^2 is the total variance of the y-variable and RMS is Residual Mean Square.

$$\text{Adjusted } (R^2) = 1 - \frac{RMS}{s_y^2} \quad (\text{Eqn. 2})$$

$$\text{Adjusted } (R^2) = 1 - \frac{(1 - R^2)(n - 1)}{(n - p - 1)} \quad (\text{Eqn. 3})$$

The Akaike Information Criterion (AIC) provides solution to the model selection by way of computing the relative quality of a given statistical model in given set of experimental data [41]. However, corrected AIC or AICc is used for data set with high number of parameter or having a smaller number of values [42]. For each data set in a model, the AICc is calculated based on the following equation (**Eqn. 4**);

$$AICc = 2p + n \ln \left(\frac{RSS}{n} \right) + 2(p+1) + \frac{2(p+1)(p+2)}{n-p-2} \quad (\text{Eqn. 4})$$

Where n and p represent number of data points in the curve and the number of parameters utilized in the model, respectively. This procedure considers variations in the number of parameters and the goodness-of-fit between two models. Perhaps, for every set of data, the model with smallest AICc value is more likely correct [42].

The Bias and Accuracy factors (BF and AF) were calculated according to Eqns. 5 and 6 to test the goodness-of-fit of the models [43]. The value of the Accuracy Factor is usually ≥ 1 , higher values signifies less precise prediction. In a bacterial growth curves or Mo-blue production, an ideal match between observed and predicted values is achieved when the Bias Factor is equal to 1. A bias factor greater than 1 signifies fail-safe model, whereas, a bias factor less than 1 signifies a fail-negative model.

$$\text{Bias factor} = 10^{\left(\frac{\sum_{i=1}^n \log \left(\frac{Pd_i}{Ob_i} \right)}{n} \right)} \quad (\text{Eqn. 5})$$

$$\text{Accuracy factor} = 10^{\left(\frac{\sum_{i=1}^n \log \left(\left| \frac{Pd_i}{Ob_i} \right| \right)}{n} \right)} \quad (\text{Eqn. 6})$$

RESULTS AND DISCUSSION

In this bacterium, the Mo-blue production profile over time gives a sigmoid-shaped with a lag phase of about 15 h. Maximum Mo-blue production occurred at around 50 h of static incubation (**Fig. 1**). Mo-blue production over time was modelled using eight different models, and all the fitting were visually acceptable (**Fig. 2**). Statistical analysis reveals Baranyi-Roberts model as the best fitting with lowest AICc and RMSE values, and highest adjusted R^2 value. The AF and BF values were equally excellent for the model with values closest to 1.0 (**Table 2**). The coefficients for the Baranyi-Roberts model at various molybdenum concentrations are shown in **Table 3**.

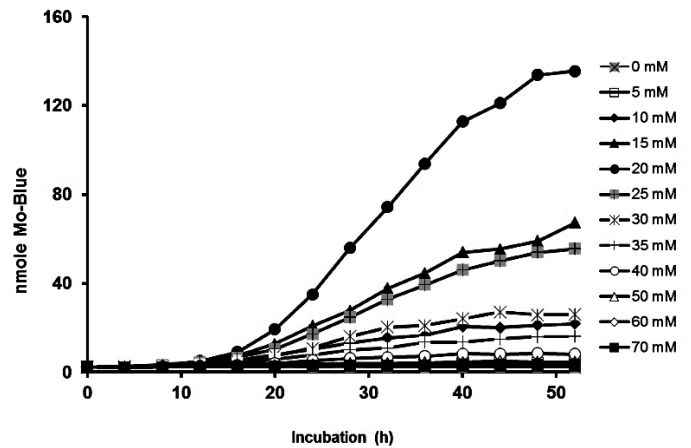


Fig. 1. Mo-blue production curves of *Bacillus* sp. strain Neni-10 at various sodium molybdate concentrations over time. Data represented as mean \pm SD of three replicates.

Table 2. Statistical analysis for various fitting models.

Model	p	RMSE	R^2	ad R^2	AICc	BF	AF
Huang	4	0.048	0.999	0.999	-64.15	1.11	1.24
Baranyi-Roberts	4	0.128	0.994	0.991	-36.66	1.20	1.27
Buchanan-3-phase	3	0.020	0.994	0.993	-94.76	1.01	1.09
modified Logistics	3	0.089	0.997	0.996	-52.55	0.99	1.20
modified Richards	4	0.022	0.992	0.990	-86.42	0.82	1.24
von Bertalanffy	3	0.101	0.996	0.994	-49.04	0.58	1.88
modified Gompertz	3	0.022	0.997	0.999	-99.79	1.01	1.01
modified Schnute	4	0.089	0.997	0.995	-47.00	1.24	1.26

Note:

- p no of parameters
- ad R^2 Adjusted Coefficient of determination
- BF Bias factor
- AF Accuracy factor

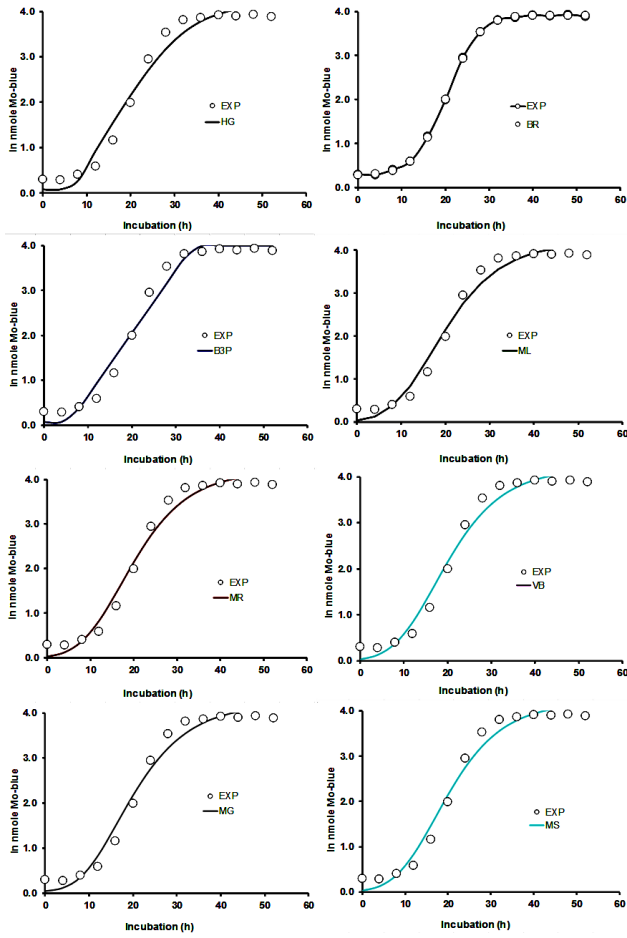


Fig. 2. Mo-blue production curve of *Bacillus* sp. strain Neni-10 at 20 mM sodium molybdate fitting various models such as Huang (HG), Baranyi-Roberts (BR), Buchanan-three phase (B3P), modified Logistics (ML), modified Richards (MR), von Bertalanffy (VB), modified Gompertz (MG) and modified Schnute (MS).

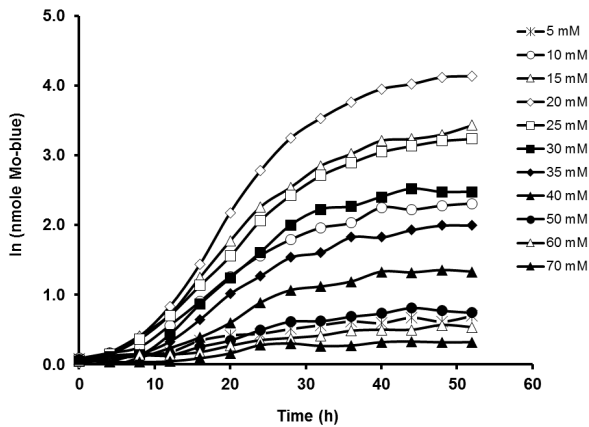


Fig. 3. Mo-blue production curves of *Bacillus* sp. strain Neni-10 on various sodium molybdate concentrations fitted Baranyi-Roberts model.

Table 3. Mo-blue production coefficients at various molybdenum concentrations modelled using Baranyi-Roberts model.

	Molybdenum concentration (mM)										
	5	10	15	20	25	30	35	40	50	60	70
Asymptote (ln nmol Mo-blue)	0.45	1.29	1.80	2.59	3.54	3.69	3.14	1.71	1.47	0.86	0.50
μ_m (h ⁻¹)	0.02	0.06	0.10	0.12	0.14	0.15	0.14	0.13	0.08	0.06	0.04
lag (h)	6.92	11.37	12.36	12.13	12.07	12.45	12.89	13.86	13.56	13.44	15.07

The Baranyi Roberts model fitted the data best by having the highest adjusted R^2 value, lowest RMSE and AICc values and the closest values to unity for both Accuracy and Bias factors. This model proposed that Eqn. 7 (first-order differential equation) describes the variation in the cell population (x) with time [44];

$$\frac{dx}{dt} = \alpha(t)\mu(x)x \tag{Eqn. 7}$$

Below is the relationship is assumed for growth or production rate (Eqn. 8)

$$\mu = \mu_{max} \left(1 - \frac{x}{x_{max}} \right) \tag{Eqn. 8}$$

The generic form of the model can be rewritten as Eqn. 9.

$$\mu(t) = \frac{1}{x(t)} \frac{dx}{dt} = \mu_{max} \alpha(t) f(t) \tag{Eqn. 9}$$

In the model, $\alpha(t)$ function assumes that growth during the lag phase was inhibited by a ‘bottle-neck’ intracellular component represented by $P(t)$ in a similar manner to the Michaelis–Menten kinetics. The quotient q_0 represented the physiological state of the inoculum, if the ratio between the substance $P(t)$ and its Michaelis–Menten constant grows exponentially, from an initial value q_0 , at a constant specific rate. The $\alpha(t)$ increases monotonously with the limits $0 \leq \alpha \leq 1$ and $\lim_{t \rightarrow \infty} \alpha(t) = 1$ as follows (Eqn. 10);

$$\alpha(t) = \frac{P(t)}{P(t) + K_p} = \frac{q(t)}{1 + q(t)} = \frac{q_0}{q_0 + e^{-\mu_{max}t}} \tag{Eqn. 10}$$

The end-of product formation or end-of-growth inhibition is represented by the $f(t)$ function (Eqn. 11), which decreases monotonically with $f(0) = 1$ and $\lim_{t \rightarrow \infty} f(t) = 0$. The $f(t)$ function is described by a logistic inhibition function in most dynamics models as follows;

$$f(t) = 1 - \left(\frac{x}{x_{max}} \right) \tag{Eqn. 11}$$

Solutions to this differential equation was successfully worked out at a certain fixed condition, e.g. isothermal temperatures. The consequence of the solution is for it to have six parameters (Eqn 12) (1);

$$y = A + \mu_{\max} x + \frac{1}{\mu_{\max}} \ln(e^{-\nu x} + e^{-h_0} - e^{-\nu x - h_0}) - \frac{1}{m} \ln \left(1 + \frac{e^{\frac{m\mu_{\max} x + 1}{\mu_{\max}} \ln(e^{-\nu x} + e^{-h_0} - e^{-\nu x - h_0})} - 1}{e^{m(y_{\max} - A)}} \right)$$

Where;

A signifies initial concentration of cell (or product concentration), y_{\max} is the asymptomatic cell concentration (or product concentration) in ln (CFU/ml) or ln product concentration, m is the curvature parameter, symbolizes the transition from the exponential phase. The h_0 is a dimensionless parameter indicating the initial physiological state of the cells, while ν is the curvature parameter that characterize the transition to the exponential phase. The maximum specific growth rate ($1/h$) is represented as μ_{\max} or μ_m and the lag time $\lambda(h)$ equals h_0/μ_{\max} .

The parameters for the curvature are; $\nu = \mu_{\max}$ or μ_m and $m=1$. Decrease in the number of parameters by two results in the model having four parameters left; μ_{\max} ; h_0 ; A and y_{\max} (Eqn. 13). Baranyi and Roberts suggested that h_0 can be considered as suitability indicator of the microbes to the true environment [1]. If the experimental method is standardized, the suitability indicator may be more or less constant, which can tally with the assumption that λ (lag time) and μ_{\max} (maximum specific growth rate) are inversely proportional.

$$y = A + \mu_{\max} x + \frac{1}{\mu_{\max}} \ln(e^{-\mu_{\max} x} + e^{-h_0} - e^{-\mu_{\max} x - h_0}) - \ln \left(1 + \frac{e^{\frac{\mu_{\max} x + 1}{\mu_{\max}} \ln(e^{-\mu_{\max} x} + e^{-h_0} - e^{-\mu_{\max} x - h_0})} - 1}{e^{(y_{\max} - A)}} \right) \quad (\text{Eqn. 13})$$

The mechanistic in attributes of the Baranyi-Roberts model was suggested to be a lot better than the modified Gompertz model, with its parameters having more biological meaning than the modified Gompertz model, in spite the fact that the model has 4 fitting parameters. The Baranyi-Roberts model was selected in fitting the growth profile of *Bacillus* sp. strain Neni-10 based on its mechanistically-inclined properties compared to modified Gompertz model (Fig. 4). It was suggested that to increase the statistical significance of a mechanistic model with 4 parameters over non-mechanistic 3-parameter model, the number of data sets obtained be raised [23].

Baranyi and Roberts model has been used successfully to model bacterial growth curves of *Brochothrix thermosphacta*, *Bacillus* spp., *Escherichia coli* O157:H7, *Clostridium* spp., *Listeria monocytogenes*, *Staphylococcus* spp., *Salmonella* Typhimurium and *Yersinia enterocolitica* [1,25,29,45,46]. This model is most preferred due to its excellent fitting capability, the model is suitable for dynamic environmental conditions, and majority of the model parameters have biological meaning [29,47]. Additionally, the Baranyi-Roberts model was used to successfully to model algal growth [48,49].

The biological meaningful coefficients gotten from the fitting process are; lag time (λ), maximal Mo-blue production (Y_{\max}) and maximum Mo-blue production rate (μ_m), which could be used for the secondary modelling of Mo-blue production using models such as two-parameter Monod or more complex secondary models like Aiba, Yano Haldane, etc. These mechanistic models are often used in basic research with the aim of gaining better understanding of the physical, chemical and biological processes that lead to the growth profile observed. All things being equal, mechanistic models are powerful tools as they

tell more about the driving patterns of the underlying processes. They are more likely to work correctly when extrapolating beyond the observed conditions [50].

CONCLUSION

The Mo-blue production in *Bacillus* sp. strain Neni-10 has been successfully modelled using eight different models, Baranyi-Roberts model was the best model fitting the Mo-blue production curve based on statistical values for RMSE (root-mean-square error), adR^2 (adjusted coefficient of determination), AICc (corrected Akaike Information Criterion), AF (accuracy factor) and BF (bias factor). Parameters obtained from the fitting exercise were maximum Mo-blue production rate (μ_m), lag time (λ) and maximal Mo-blue production (Y_{\max}) of X (h^{-1}), Y (h) and Z (nmol Mo-blue), respectively. In heavy metals detoxification process by microbes, the use of growth curve models to get accurate Mo-blue production rate that could be utilized further for secondary modelling is novel as demonstrated by literature search. This work has therefore established the applicability of such models. Work is still ongoing to conduct secondary modelling on the inhibitory effects of substrate (molybdenum), pH and temperature on maximum Mo-blue production rate.

REFERENCES

1. Baranyi J, Roberts TA. A dynamic approach to predicting bacterial growth in food. *Int J Food Microbiol.* 1994;23(3-4):277-94.
2. Buchanan RL, Whiting RC, Damert WC. When is simple good enough: A comparison of the Gompertz, Baranyi, and three-phase linear models for fitting bacterial growth curves. *Food Microbiol.* 1997;14(4):313-26.
3. Neunhuserer C, Berreck M, Insam H. Remediation of soils contaminated with molybdenum using soil amendments and phytoremediation. *Water, Air, and Soil Pollut.* 2001;128(1-2):85-96.
4. Underwood EJ. Environmental sources of heavy metals and their toxicity to man and animals. 1979;11(4-5):33-45.
5. Kincaid RL. Toxicity of ammonium molybdate added to drinking water of calves. *J Dairy Sci.* 1980;63(4):608-10.
6. Shukor MY, Habib SHM, Rahman MFA, Jirangon H, Abdullah MPA, Shamaan NA, et al. Hexavalent molybdenum reduction to molybdenum blue by *S. Marcescens* strain Dr. Y6. *Appl Biochem Biotechnol.* 2008;149(1):33-43.
7. Rahman MFA, Shukor MY, Suhaili Z, Mustafa S, Shamaan NA, Syed MA. Reduction of Mo(VI) by the bacterium *Serratia* sp. strain DRY5. *J Environ Biol.* 2009;30(1):65-72.
8. Lim HK, Syed MA, Shukor MY. Reduction of molybdate to molybdenum blue by *Klebsiella* sp. strain hkeem. *J Basic Microbiol.* 2012;52(3):296-305.
9. Abo-Shakeer LKA, Ahmad SA, Shukor MY, Shamaan NA, Syed MA. Isolation and characterization of a molybdenum-reducing *Bacillus pumilus* strain Iba. *J Environ Microbiol Toxicol.* 2013;1(1):9-14.
10. Othman AR, Bakar NA, Halmi MIE, Johari WLW, Ahmad SA, Jirangon H, et al. Kinetics of molybdenum reduction to molybdenum blue by *Bacillus* sp. strain A.rzi. *Biomed Res Int.* 2013;2013:Article number 371058.
11. Mansur R, Gusmanizar N, Roslan MAH, Ahmad SA, Shukor MY. Isolation and characterisation of a molybdenum-reducing and Metanil yellow dye-decolourising *Bacillus* sp. strain Neni-10 in soils from West Sumatera, Indonesia. *Trop Life Sci Res.* 2017 Jan;28(1):69-90.
12. Kesavan V, Mansur A, Suhaili Z, Salihan MSR, Rahman MFA, Shukor MY. Isolation and Characterization of a Heavy Metal-reducing *Pseudomonas* sp. strain Dr.Y Kertih with the Ability to Assimilate Phenol and Diesel. *Bioremediation Sci Technol Res.* 2018 Jul;6(1):14-22.
13. Maarof MZ, Shukor MY, Mohamad O, Karamba KI, Halmi MIE, Rahman MFA, et al. Isolation and Characterization of a Molybdenum-reducing *Bacillus amyloliquefaciens* strain KIK-12

- in Soils from Nigeria with the Ability to grow on SDS. *J Environ Microbiol Toxicol*. 2018 Jul;6(1):13–20.
14. Campbell AM, Del Campillo-Campbell A, Villaret DB. Molybdate reduction by *Escherichia coli* K-12 and its chl mutants. *Proc Natl Acad Sci U S A* [Internet]. 1985;82(1):227–31.
 15. Capaldi A, Proskauer B. Beiträge zur Kenntniss der Säurebildung bei Typhus-bacillen und *Bacterium coli* - Eine differential-diagnostische Studie. *Zeitschrift für Hyg und Infect*. 1896;23(3):452–74.
 16. Khan A, Halmi MIE, Shukor MY. Isolation of Mo-reducing bacterium in soils from Pakistan. *J Environ Microbiol Toxicol*. 2014;2(1):38–41.
 17. Levine VE. The reducing properties of microorganisms with special reference to selenium compounds. *J Bacteriol*. 1925;10(3):217–63.
 18. Yamaguchi S, Miura C, Ito A, Agusa T, Iwata H, Tanabe S, et al. Effects of lead, molybdenum, rubidium, arsenic and organochlorines on spermatogenesis in fish: Monitoring at Mekong Delta area and in vitro experiment. *Aquat Toxicol*. 2007;83(1):43–51.
 19. Zhang Y-L, Liu F-J, Chen X-L, Zhang Z-Q, Shu R-Z, Yu X-L, et al. Dual effects of molybdenum on mouse oocyte quality and ovarian oxidative stress. *Syst Biol Reprod Med*. 2013;59(6):312–8.
 20. Halmi MIE, Ahmad SA, Syed MA, Shamaan NA, Shukor MY. Mathematical modelling of the molybdenum reduction kinetics in *Bacillus pumilus* strain Lbna. *Bull Environ Sci Manag*. 2014;2(1):24–9.
 21. Othman AR, Bakar NA, Halmi MIE, Johari WLW, Ahmad SA, Jirangon H, et al. Kinetics of molybdenum reduction to molybdenum blue by *Bacillus* sp. strain A.rzi. *Biomed Res Int*. 2013;2013:1–9.
 22. Gompertz B. On the nature of the function expressive of the law of human mortality, and on a new mode of determining the value of life contingencies. 1825;115:513–85.
 23. Zwietering MH, Jongenburger I, Rombouts FM, Van't Riet K. Modeling of the bacterial growth curve. *Appl Environ Microbiol*. 1990;56(6):1875–81.
 24. Ricker, F.J. 11 Growth Rates and Models. In: W.S. Hoar DJR and JRB, editor. *Fish Physiology*. Academic Press; 1979. p. 677–743. (Bioenergetics and Growth; vol. Volume 8).
 25. Baranyi J. Mathematics of predictive food microbiology. *Int J Food Microbiol*. 1995;26(2):199–218.
 26. Richards, F.J. A flexible growth function for empirical use. *J Exp Bot*. 1959;10:290–300.
 27. Buchanan RL. Predictive food microbiology. *Trends Food Sci Technol*. 1993;4(1):6–11.
 28. Babák L, Šupinová P, Burdychová R. Growth models of *Thermus aquaticus* and *Thermus scotoductus*. *Acta Univ Agric Silvicae Mendelianae Brun*. 2012;60(5):19–26.
 29. López S, Prieto M, Dijkstra J, Dhanoa MS, France J. Statistical evaluation of mathematical models for microbial growth. *Int J Food Microbiol*. 2004;96(3):289–300.
 30. Huang L. Optimization of a new mathematical model for bacterial growth. *Food Control*. 2013;32(1):283–8.
 31. Shukor MS, Shukor MY. A microplate format for characterizing the growth of molybdenum-reducing bacteria. *J Environ Microbiol Toxicol*. 2014;2(2):1–3.
 32. Ghani B, Takai M, Hisham NZ, Kishimoto N, Ismail AKM, Tano T, et al. Isolation and characterization of a Mo⁶⁺-reducing bacterium. 59(4):1176–80.
 33. Shukor Y, Adam H, Ithnin K, Yunus I, Shamaan NA, Syed A. Molybdate reduction to molybdenum blue in microbe proceeds via phosphomolybdate intermediate. *J Biol Sci*. 2007;7(8):1448–52.
 34. Rahman MFA, Shukor MY, Suhaili Z, Mustafa S, Shamaan NA, Syed MA. Reduction of Mo(VI) by the bacterium *Serratia* sp. strain DRY5. *J Environ Biol*. 2009;30(1):65–72.
 35. Lim HK, Syed MA, Shukor MY. Reduction of molybdate to molybdenum blue by *Klebsiella* sp. strain hkeem. *J Basic Microbiol*. 2012;52(3):296–305.
 36. Abo-Shakeer LKA, Ahmad SA, Shukor MY, Shamaan NA, Syed MA. Isolation and characterization of a molybdenum-reducing *Bacillus pumilus* strain lbna. *J Environ Microbiol Toxicol*. 2013;1(1):9–14.
 37. Ahmad SA, Shukor MY, Shamaan NA, Mac Cormack WP, Syed MA. Molybdate reduction to molybdenum blue by an antarctic bacterium. *Biomed Res Int*. 2013;(December):1–10.
 38. Halmi MIE, Zuhainis SW, Yusof MT, Shaharuddin NA, Helmi W, Shukor Y, et al. Hexavalent molybdenum reduction to Mo-blue by a Sodium-Dodecyl-Sulfate-degrading *Klebsiella oxytoca* strain DRY14. *Biomed Res Int*. 2013;2013:e384541.
 39. Shukor MY, Lee CH, Omar I, Karim MIA, Syed MA, Shamaan NA. Isolation and characterization of a molybdenum-reducing enzyme in *Enterobacter cloacae* strain 48. *Pertanika J Sci Technol*. 2003;11(2):261–72.
 40. Motulsky HJ, Ransnas LA. Fitting curves to data using nonlinear regression: a practical and nonmathematical review. *FASEB J*. 1987;1(5):365–74.
 41. Akaike H. New look at the statistical model identification. *IEEE Trans Automat Contr*. 1974;AC-19(6):716–23.
 42. Burnham KP, Anderson DR. *Model Selection and Multimodel Inference: A Practical Information-Theoretic Approach*. Springer Science & Business Media; 2002. 528 p.
 43. Ross T, McMeekin TA. Predictive microbiology. *Int J Food Microbiol*. 1994;23(3–4):241–64.
 44. Perni S, Andrew PW, Sharma G. Estimating the maximum growth rate from microbial growth curves: definition is everything. *Food Microbiol*. 2005;491–495(6):491–5.
 45. Coleman ME, Tamplin ML, Phillips JG, Marmer BS. Influence of agitation, inoculum density, pH, and strain on the growth parameters of *Escherichia coli* O157:H7 - Relevance to risk assessment. *Int J Food Microbiol*. 2003;83(2):147–60.
 46. Fujikawa H. Development of a new logistic model for microbial growth in foods. *Biocontrol Sci*. 2010;15(3):75–80.
 47. Van Impe JF, Poschet F, Geeraerd AH, Vereecken KM. Towards a novel class of predictive microbial growth models. *Int J Food Microbiol*. 2005;100(1–3):97–105.
 48. Lacerda LMCF, Queiroz MI, Furlan LT, Lauro MJ, Modenesi K, Jacob-Lopes E, et al. Improving refinery wastewater for microalgal biomass production and CO₂ biofixation: Predictive modeling and simulation. *J Pet Sci Eng*. 2011;78(3–4):679–86.
 49. Tevatia R, Demirel Y, Blum P. Kinetic modeling of photoautotrophic growth and neutral lipid accumulation in terms of ammonium concentration in *Chlamydomonas reinhardtii*. *Bioresour Technol*. 2012;119:419–24.
 50. Bolker BM. *Ecological Models and Data in R*. Princeton, N.J: Princeton University Press; 2008. 408 p.